CLM - R 192

CLM - R 192

UKAEA

Report

HOLOGRAPHIC INTERFEROMETRY OF ISOLATED DEUTERIUM PLASMAS PRODUCED BY A CO_2 LASER

P V GATENBY
A C WALKER

CULHAM LABORATORY
Abingdon Oxfordshire

1979

C18

Available from H. M. Stationery Office

£1.00

CLM-R 192

HOLOGRAPHIC INTERFEROMETRY OF ISOLATED DEUTERIUM PLASMAS PRODUCED BY A CO_2 LASER

P.V. Gatenby and A.C. Walker
Culham Laboratory, Abingdon, Oxon., OX14 3DB, UK
(Euratom/UKAEA Fusion Association)

ABSTRACT

The application of double exposure fractional fringe holographic interferometry to measurements of electron density in a plasma generated by irradiation of a freely falling pellet of solid deuterium with a focused CO_2 laser pulse is discussed. A particularly simple technique is used for processing and reconstructing the holograms and this is described in detail. A summary and discussion of the results is included with the emphasis on the observed evolution of the deuterium plasma over the duration of the laser irradiation.

.....

October 1978.

SBN 85311 075 1

1. INTRODUCTION

Techniques for determining the electron density distribution in transient plasmas by means of holographic interferometry are now widespread.[1] The present work was undertaken as part of a programme for filling CLEO stellarator with a laser produced deuterium plasma. Previous studies of a similar kind have been reported for irradiation of suspended polythene pellets by CO_2 laser[2] and for staged heating of polyethylene filaments by a combination of Nd:glass and CO_2 lasers.[3] Holographic interferometry of isolated deuterium plasma obtained by irradiation of freely falling pellets with a focused Nd:glass laser has also been reported.[4] In some respects the present work is complementary to the latter.

The holographic technique itself involves taking two sequential holograms on the same photographic emulsion, one exposure having the plasma present and the other providing a reference. Upon reconstruction, two superimposed wavefronts are generated and the phase differences introduced between these by the plasma give rise to an interference pattern analogous to that from a conventional interferometer. This technique however has a great advantage over the latter in that the interfering beams traverse the same path, thus dispensing with the need for high quality optics and critical alignment. There are two basic configurations for producing holographic interferograms.[5] In the one most analogous to conventional diffuse reflection holography of opaque objects, a ground glass diffuser is located in the scene beam (that traversing the target chamber). Each point on the diffuser then illuminates every point on the holographic plate giving a three dimensional record of the object. By removing the diffuser, a one to one correspondence between test section and holographic plate is obtained but the three dimensional information is lost. On the other hand, better resolution is obtained due to elimination of the speckle pattern associated with the ground glass screen. This latter technique, outlined in an earlier Culham Report[6] has been adopted and improved upon for the present work.

2. EXPERIMENTAL ARRANGEMENT

The experimental arrangement employed for holographic interferometry is shown in Fig.1. The ruby laser consisted of a Q-switched Korad oscillator with a plane-plane cavity configuration and provided pulses of 20 ns duration (FWHM). No intracavity stops were used to limit transverse mode structure but instead a central region of the beam about 1 mm in diameter

was expanded by a factor of 20 to provide a spatially coherent source. The beam was split so that 50% traversed the target chamber and the remainder was directed on to the holographic plate by means of a plane mirror which could be tilted by a controlled amount through the use of a heated wire mechanism.[6] The mirror was tilted through a small angle between exposures, introducing a set of background (wedge) fringes, which facilitate analysis of the interferogram.[7] A 20 cm focal length lens was used to image the plasma on to the holographic plate. This imaging counteracts the refractive bending effects of the plasma due to transverse refractive index gradients, which otherwise would degrade the interference fringe pattern and image of the plasma. An important requirement of the holographic set-up is that the scene beam and reference beam path lengths must be matched to within the coherence length of the ruby laser ($\tilde{-}$ 40 mm) and a compensating lens was included in the reference beam to ensure this. Additionally, inclusion of this lens facilitates the exact superposition of scene and reference beams on the holographic plate and eases the requirement for spatial coherence. A red filter prevented shorter wavelength light emission from the plasma and stray light in the laboratory from reaching the holographic plate.

Solid deuterium targets were dropped from a Leybold-Heraeus cryosource, based on a prototype developed at IPP Garching.[8] The pellets were formed by extruding a rod of frozen deuterium with a radius of ~ 150 μm through an orifice and cutting off a suitable length using two symmetrically arranged ohmically heated wires. The pellets were allowed to fall freely under gravity until detected and hit by the focused pulse from an electron beam sustained atmospheric pressure CO_2 laser (TROJAN). The CO_2 and ruby lasers were triggered by photodiodes monitoring the obscuration of two HeNe probe beams by the falling pellet. The first probe beam, positioned ~ 2.5 mm above the focal point of the CO_2 laser, was used to fire the ruby laser flashlamps and the second, aligned on the focal point, triggered the main CO_2 laser followed by the ruby laser Q-switch after a suitable delay. This delay enabled the ruby laser to be fired at different intervals after the onset of the CO_2 pulse, allowing a series of time resolved measurements of the plasma refractivity to be made. The field of view of the holographic plate was increased from 1 cm^2 to 8 cm^2 for late delay times so that more of the expanding plasma could be observed.

3. PROCESSING AND RECONSTRUCTION OF THE HOLOGRAMS

Holograms were recorded on Agfa-Gevaert 10E75 plates. These require an exposure of order 6 $\mu J\ cm^{-2}$ and provide a resolution of 2800 lines mm^{-1}. The exposed plates may be processed to produce either amplitude or phase holograms. The latter modulate the reconstruction beam by changes in the dielectric constant or thickness of the emulsion and, because they can in principle be lossless diffracting structures, their diffraction efficiencies can be much higher than those of amplitude holograms. Phase holograms however require extra steps in processing, in particular a bleaching procedure. For simplicity, the present study used amplitude holograms with reconstruction by reflection.[9] This technique relies on the photographic relief image which appears in the emulsion after processing[10] and enables the hologram to be used as a phase modulator while only requiring the processing of an amplitude hologram. The method also allows the production of good quality holograms within a large range of exposures, thus making the ruby laser intensity less critical.

Processing was found to be very insensitive to the precise procedure employed and the following simple method produced excellent results. Plates were first developed for 5 minutes in Agfa G3p developer, washed, fixed for 5 minutes in Agfa G321 (Structurix), washed again and finally allowed to dry. After the holograms dried, fringes could be viewed by reflection from the emulsion side in ambient light, and could clearly be seen to be localized in the plane of the hologram from their lack of parallax.

In general, the reconstruction of a hologram gives rise to two wavefronts which may both be convergent, both divergent, or one of each type and these may be considered to correspond to image points at co-ordinates (Xi, Yi, Zi). Suppose the object wave is generated by a point source at (Xo, Yo, Zo) and the reference wave by a point source at (Xr, Yr, Zr) of wavelength λ_1. If the reconstruction wave originates at point (Xc, Yc, Zc) and has a wavelength λ_2, then for reconstruction by reflection

$$Xi = \pm \frac{\lambda_2\ Zi\ Xo}{\lambda_1\ Zo} \mp \frac{\lambda_2\ Zi\ Xr}{\lambda_1\ Zr} - \frac{Zi\ Xc}{Zc} \qquad \ldots(1a)$$

$$Yi = \pm \frac{\lambda_2\ Zi\ Yo}{\lambda_1\ Zo} \mp \frac{\lambda_2\ Zi\ Yr}{\lambda_1\ Zr} - \frac{Zi\ Yc}{Zc} \qquad \ldots(1b)$$

$$Zi = -\left[\frac{1}{Zc} \pm \frac{\lambda_2}{\lambda_1}\left\{\frac{1}{Zr} - \frac{1}{Zo}\right\}\right]^{-1} \qquad \ldots(1c)$$

where the upper set of signs corresponds to one wavefront and the lower set to the other. From equation (1c) it may be seen that when

$$\frac{1}{Zc} > \frac{\lambda_2}{\lambda_1}\left\{\frac{1}{Zr} - \frac{1}{Zo}\right\}$$

two divergent wavefronts will be produced while for the inverse case, one convergent and one divergent wavefront will result.

Reconstruction of the holograms could be achieved most conveniently using a HeNe laser, so that $\lambda_1 \simeq \lambda_2$. The optical arrangement is shown in Fig.2. The holographic plate was imaged on to Polaroid film using first order diffracted light. The HeNe laser beam was expanded and spatially filtered to improve spatial coherence and beam quality. Where possible, a convergent reconstructed wavefront was used because this could most easily be collected by the 20 cm focal length lens. Good results were also obtained using incoherent white light in place of the HeNe laser beam by imaging the first order spectrum on to the film. Image quality however, was limited by the wavelength dependence of the reconstruction process and by chromatic aberrations in the focusing lens.

4. ANALYSIS

The interpretation of holographically produced interferograms is equivalent to that of the fringe patterns produced by conventional interferometry. The effective change due to the plasma in units of fringe spacings is given by

$$p = \int [(\mu - 1)/\lambda]\, d\ell \qquad \ldots(2)$$

where $d\ell$ is an element of path length along the line of sight and μ is the refractive index of the plasma. In general, free electrons, ions and neutral particles in various states of excitation, will each contribute to the plasma refractivity so that

$$(\mu - 1) = \sum_j K_j n_j \qquad \ldots(3)$$

where K_j is the particle refractivity of species j and n_j is the number concentration. Thus, for a particular species, the line density is given by

$$\int n_j(\ell).d\ell = (\lambda/K_j)p_j \qquad \ldots(4)$$

For electrons (λ = 0.6943 μm)[11] $\quad \lambda/Ke = \frac{-2\pi mc^2}{e^2\lambda} = 3.2 \times 10^{17} cm^{-2}$

For molecular D_2 (neutral, ground state) $\quad \lambda/K_{D2} = \frac{\lambda n_{D2}}{\mu_{D2}-1} = 1.4 \times 10^{19} cm^{-2}$

For atomic D (neutral, ground state) $\quad \lambda/K_D = \frac{\lambda n_{D2}}{\mu_D-1} = 1.7 \times 10^{19} cm^{-2}$

where the published value of refractive index, μ_{D2}[12] is used and the published ratio of the polarizability of atomic and molecular hydrogen[13] is assumed applicable to deuterium. Other species include the deuterium ion, which can be neglected due to its small contribution being always dominated by the electronic component in a neutral plasma, and the various excited states of neutral deuterium. These latter contributions will also be small except when the probe wavelength is close to a resonant transition. To distinguish these various components multiwavelength interferometric techniques must be employed. However, for this study it is assumed that the high sensitivity to electrons ensures that these are the dominant contribution to the observed fringe shifts. Any region with an excess of neutral material is recognised by fringe shifts in the opposite direction. The direction of fringe shifts was calibrated from a reference interferogram of a helium gas jet in air.

The most simply derived quantity is the total number of electrons in the field of view obtained by integrating over the area of the interferogram. This does not require any assumptions about the variation of n_e with ℓ. In order to obtain information on the distribution of electron densities in the plasma however, cylindrical symmetry must be assumed in order to perform Abel inversions on the interferometric data. (The alternative is multidirectional interferometry together with the associated complex analysis.) A computer program based on the inversion procedure and coefficients described by Bockasten[14] has been used to generate the radial profiles on a 21 point grid.

5. RESULTS AND DISCUSSION

Over 20 holographic interferograms of the interaction between D_2 pellets and CO_2 laser pulses have been taken. The pellets were typically of the form shown in Fig.3 and contained 2-4 x 10^{18} deuterium atoms. The

CO_2 laser pulses were of energy 1.3 - 1.5 kJ in a 50 ns (FWHM) gain switched spike plus tail of duration ~ 2 μs and around one eighth of the peak power. The irradiance averaged over the pellet dimensions was of order 6 x 10^{11} W cm^{-2} at the peak of the pulse, with a central maximum value of 1.8 x 10^{12} W cm^{-2}. Figs.(4) and (5) show a sequence of interferograms taken at various times during the pellet irradiation. A summary of the quantitative information obtained from these is given in Table 1. The three earlier interferograms show a central region with no detectable fringes, which will be referred to as the 'core'. The electron densities measured close to the edge of this core are always within an order of magnitude of the critical density for 10 μm radiation (10^{19} cm^{-3}). The lack of clearly discernible fringes in the core could be caused either by turbulence or by a supercritical plasma density (for the ruby laser wavelength). The latter explanation is only consistent with conservation of the initial particle number if one assumes that the core has a foam-like structure rather than it being uniformly over-dense. The remaining possibility, that the central obscuration is due to refractive deviation of the ruby laser radiation beyond the collecting angle of the optics, has been eliminated using the CUPID[15] ray tracing program. This shows that the measured transverse refractive index gradients are too low to produce sufficient deflection of the radiation. It is concluded that the core represents the remaining non-ablated pellet material and hence we take its evolution in time as a measure of the pellet 'burn-up'. Fig.6 shows this variation of the mean core diameter with time taken from 17 interferograms. It can be seen that, after a period of expansion, the core dimensions shrink until burn-up is typically completed at the end of the 2 μs laser pulse.

Fig.4 shows the plasma at an early stage, 30 ns after the peak of the initial spike. It can be seen to extend around the sides of the pellet while at the back (away from the laser) neutral material, responsible for the sharp drop in fringe shifts, can be seen being ejected. At this time the electron density scale lengths are quite short; for example, 60 μm along the symmetry axis on the incident side of the pellet. Integration over the full area of this interferogram gives a total number of 1.6 x 10^{15} electrons although a further undetected component lies within, or is obscured by, the core.

Fig.5(a) is an interferogram taken near the middle of the laser pulse duration, and is typical of the laser pellet interaction at this stage. Abel inversion of 18 radial scans across it permit the construction of an electron isodensity contour plot for the plasma (Fig.7). It can be seen that although neutral material is still evident behind the core, the coronal plasma has extended completely around the target (due to conduction), despite the single sided illumination. The electron density profile for a scan along the axis of symmetry is shown in Fig.8. The scale length at the front of the plasma has increased to 380 μm while at the sides, in the radial direction, it is of order 700 μm. The total number of detected electrons is 4.4×10^{16}.

Figs.5(b) and 5(c) show the plasma near the end of the laser pulse. At this stage the density scale lengths are sufficiently long to produce detectable fringe shifts over a relatively large area. A core of about 1.2 mm diameter is still visible in Fig.5(b) while in the later interferogram, Fig.5(c) (which has a more closely spaced set of reference fringes for increased resolution) no core can be seen. The number of detectable electrons is around 3×10^{17} in both interferograms.

From these results certain conclusions can be drawn regarding the fractional ionization of the pellet. This parameter is of importance if, as is planned, laser produced D_2 plasma is used to fill a magnetic trap. Any remaining neutral gas may cool the confined plasma via charge exchange processes. However, an estimate of the final pellet ionization from a single interferogram is difficult due to the long irradiation time involved. Thus, plasma generated at the beginning of the pulse, which has a directed ion energy greater than 100 eV (measured by ion detectors), will have expanded to a diameter exceeding 80 cm by the end of the pulse. Detection of such large, low density, plasmas are beyond the scope of this interferometric technique. However, lower limits can be deduced from the results described so far. Fig.5(b) for example shows a plasma containing 10% of the initial pellet material within the field of view. Clearly, a higher total ionization must be concluded given that irradiation of the core continues after the time of the interferogram and that the expanded component must also be added. Combining the sequence of interferograms with measured plasma expansion velocities provides further information. Thus, taking the mean diameter of detectable plasma to be ~ 6 mm and the mean

number of electrons within it to be 5×10^{16} (averaged in each case over the laser pulse duration) then the expansion velocity of 10^7 cm sec^{-1} is consistent with total pellet ionization within 2 μs. However, the complete plasma does not necessarily all move at the expansion velocity, for which reason a more definite conclusion cannot be reached. Instead we must return to the interferograms to look for any remaining un-ionized pellet material. At times greater than 2.1 μs after the start of the CO_2 laser pulse, ie after the pulse has ended, very little material is observed on the interferograms. For example, Fig.5(d) taken at 2.8 μs shows only a small region (upper right hand side) of neutral material corresponding to less than 2% of the initial pellet. However, as has already been noted, the sensitivity of the 0.6943 μm interferometry to neutral deuterium is low. Thus, if one assumes a maximum expansion velocity of 10^5 cm sec^{-1} for neutral material and puts a lower limit to the observable fringe shifts of 0.2 of a fringe spacing, then 25% of the initial pellet could expand uniformly from the beginning of the laser pulse and be of too low a density to be detected at the time of this interferogram. Further, fragmentation (observed when lower energy laser pulses are used) could conceivably cause a number of similar undetectable regions of neutral material to evolve in different areas. However, other interferograms taken closer to the end of the laser pulse and with larger fields of view, give no indication of such significant quantities of neutral material remaining.

It is concluded that the fractional ionization must be better than 10% and could be approaching 100%. Faraday cup ion measurements raise the minimum value to 20%. If the actual ionization is near this minimum value the un-ionized material must move with the expanding plasma to explain the lack of neutral remnants after the completion of the pellet burn-up.

Finally, it is worth comparing these results with those obtained at IPP Garching by Baumhacker et al[8] using a Nd:glass laser and similar D_2 pellets. The reported ionization of only 5-10% and the clearly visible core remaining in their interferograms after the end of the laser pulse illustrate the effectiveness in the current experiments of longer duration and higher energy CO_2 laser pulses.

6. CONCLUSIONS

The measurement of electron densities in an expanding laser-produced D_2 plasma using double-exposure holographic interferometry has been described. The use of a reflection reconstruction technique with a standard plate development procedure avoids the practical complications of preparing phase holograms. The application of this technique to study the heating of isolated solid D_2 pellets with kilojoule CO_2 laser pulses suggests that complete target burn-up can be achieved in ~ 2 μs. Electron and neutral particle numbers deduced from the interferograms are consistent with high fractional ionization of the pellets.

ACKNOWLEDGEMENTS

The authors wish to acknowledge the contributions of Dr. S. Kogoshi in assisting with the commissioning and operation of the D_2 pellet source; Dr. T. Stamatakis in general experimental collaboration and Dr. I.J. Spalding in initiating this work. Messrs. S. Ward and B. Willis provided valuable technical assistance. The inversion computer program was a modified version of a program written by Dr. P. Morgan.

REFERENCES

1. JAHODA, F.C. - 'Pulse laser holographic interferometry', Modern Optical Methods in Gas Dynamic Research, Ed. D.S. Dosanjh, pp.137-154, Plenum Press, 1971.

2. WALKER, A.C., STAMATAKIS, T., SPALDING, I.J. - 'Heating of polyethylene pellets with kilojoule microsecond duration CO_2 laser pulses', to be published, J.Phys.D:Appl.Phys.11, 1978.

3. PECHACEK, R.E., GREIG, J.R. - 'Production of large warm plasmas by staged laser heating of solid targets', NRL Memorandum Report 3457, Feb.1977.

4. BAUMHACKER, H., BRINKSCHULTE, H., LANG, R.S., RIEDMULLER, W., SALVAT, M. - 'Plasma production by irradiating freely falling deuterium pellets with a high power laser', Appl.Phys.Lett.30, No.9, pp.461-463, 1977.

5. JAHODA, F.C., SIEMON, R.E. - 'Holographic interferometry cookbook', Los Alamos Report LA-5058-MS, Oct.1972.

6. ELKERBOUT, A.C.H., VAN DIJK, J.W., DONALDSON, T.P. - 'Holography of a CO_2 laser generated plasma', Culham Report CLM-R154, Dec.1975.

7. JAHODA, F.C., JEFFRIES, R.A., SAWYER, G.A. - 'Fractional-fringe holographic plasma interferometry', Appl.Optics 6, pp.1407-1410, 1967.

8. BAUMHACKER, H., BRINKSCHULTE, H., LANG, R.S., RIEDMULLER, W. - 'Experiments for filling magnetic confinement machines with laser produced plasmas. Preliminary results', Proc.9th Symp.on Fusion Technology, Garmisch - Partenkirchen, pp.873-878, Pergamon Press, 1976.

9. BRANDT, G.B., RIGLER, A.K. - 'Reflection holograms of focused images', Phys.Lett.25A, pp.68-69, 1967.

10. SMITH, H.M. - 'Photographic relief images', J.Opt.Soc.Am.58, No.4, pp.533-539, 1968.

11. JAHODA, F.C., SAWYER, G.A. - 'Optical refractivity of plasmas', Methods of Experimental Physics 9B, Ed.R.H. Lovberg, pp.1-48, 1971.

12. KAYE, G.W.C., LABY, T.H. - Tables of Physical and Chemical Constants, 14th Edition, Longman Group Ltd. (New York), p.87, 1973.

13. MARLOW, W.C., BERSHADER, D. - Phys.Rev.133, p.A629, 1964.

14. BOCKASTEN, K. - 'Transformation of observed radiances into radial distribution of the emission of a plasma', J.Opt.Soc.Am.51, pp.943-947, 1961.

15. HUBBARD, M., MONTES, A. - 'A ray tracing program for continuously varying refractive media', CLM-R189, 1978.

TABLE 1 Summary of quantitative information obtained from three typical interferograms taken at different intervals after the start of the CO_2 laser pulse.

Interval after start of CO_2 laser pulse	80 ns	0.7 μs	1.2 μs
Total number of detectable electrons	1.6×10^{15}	4.4×10^{16}	3.1×10^{17}
Fraction of deuterium atoms ionized (lower limit)	5.3×10^{-4}	1.4×10^{-2}	0.10
Maximum observable electron density at the front of the pellet (cm^{-3})	5.4×10^{18}	4.76×10^{18}	1.52×10^{18}
Scale length at the front of the pellet (μm)	60	380	2500

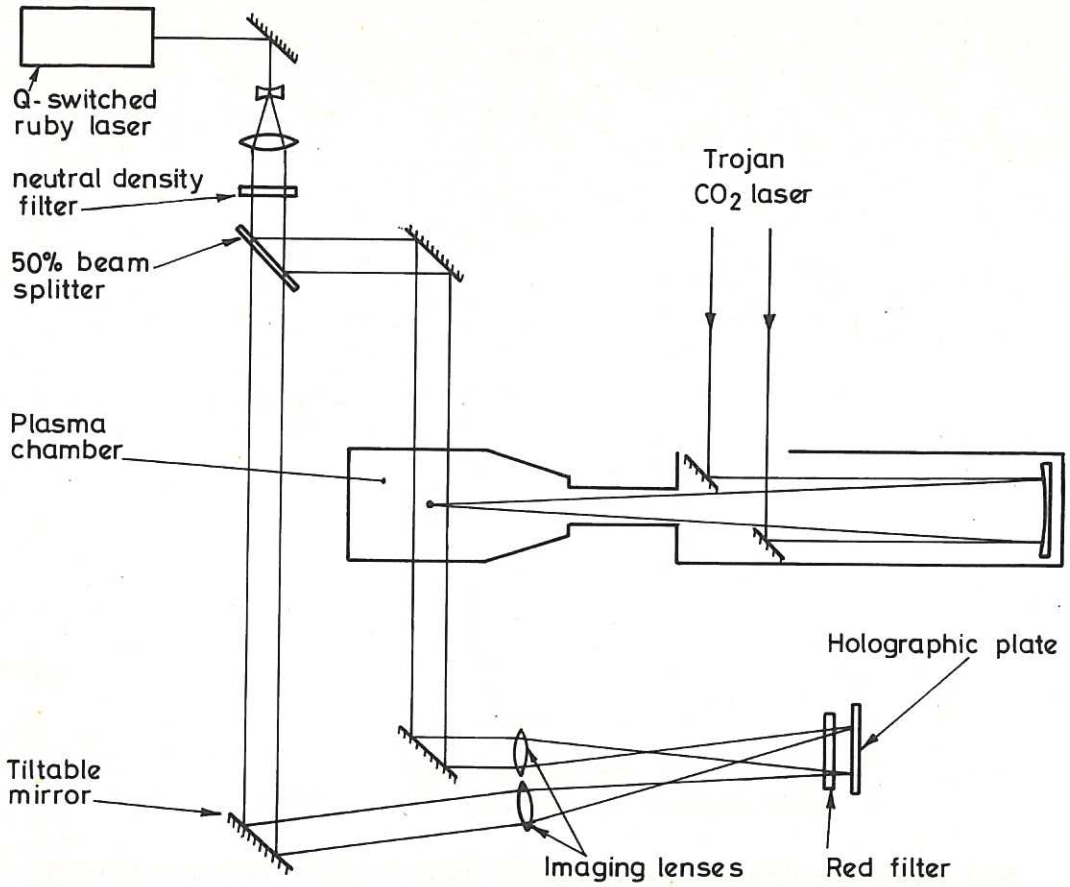

Fig.1 Schematic diagram of the experimental arrangement for holographic interferometry.

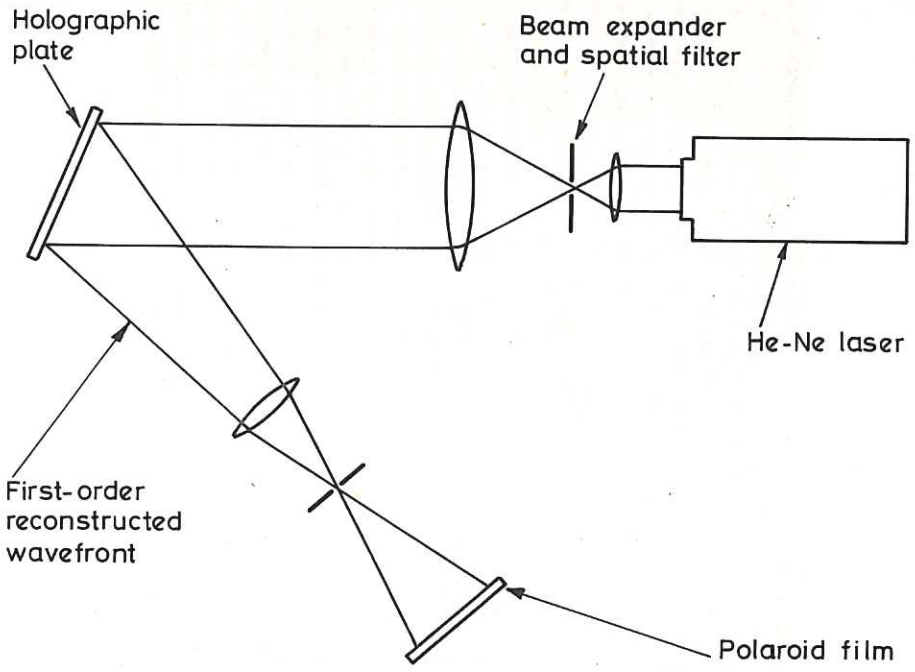

Fig.2 Optical arrangement for reconstruction of holographic interferograms.

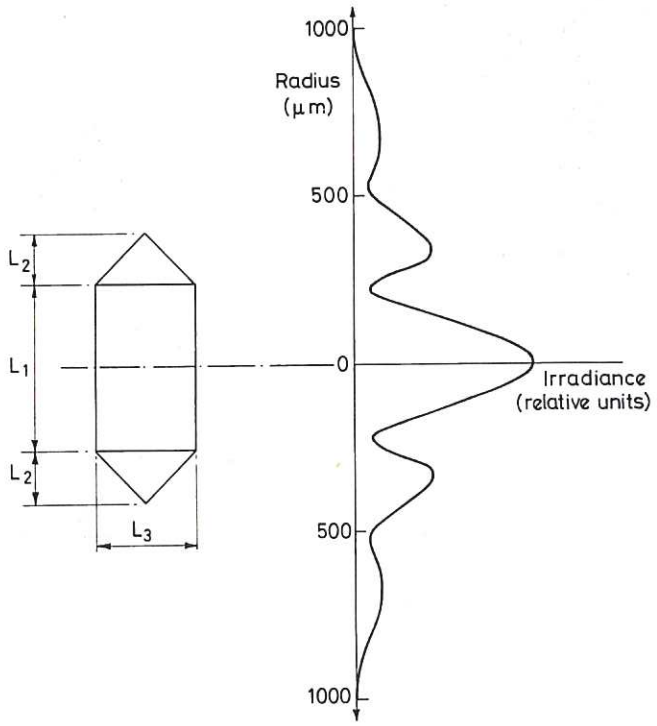

Fig.3 Typical form of the freely falling D_2 pellets and the irradiance distribution of the CO_2 laser pulses incident on the pellets.

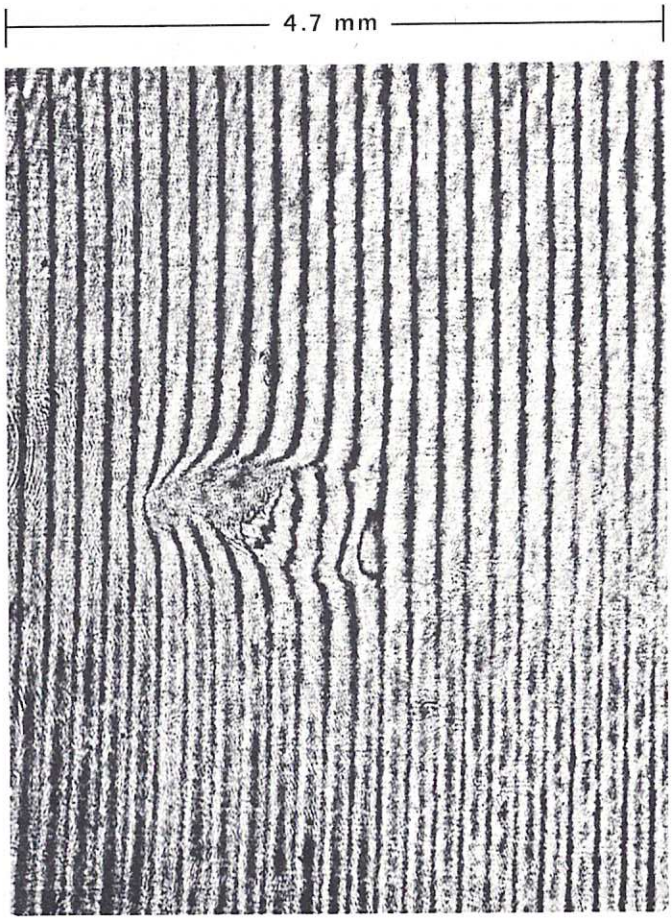

Fig.4 Interferogram of D_2 plasma 80ns from start of TROJAN pulse (CO_2 laser incident from left).

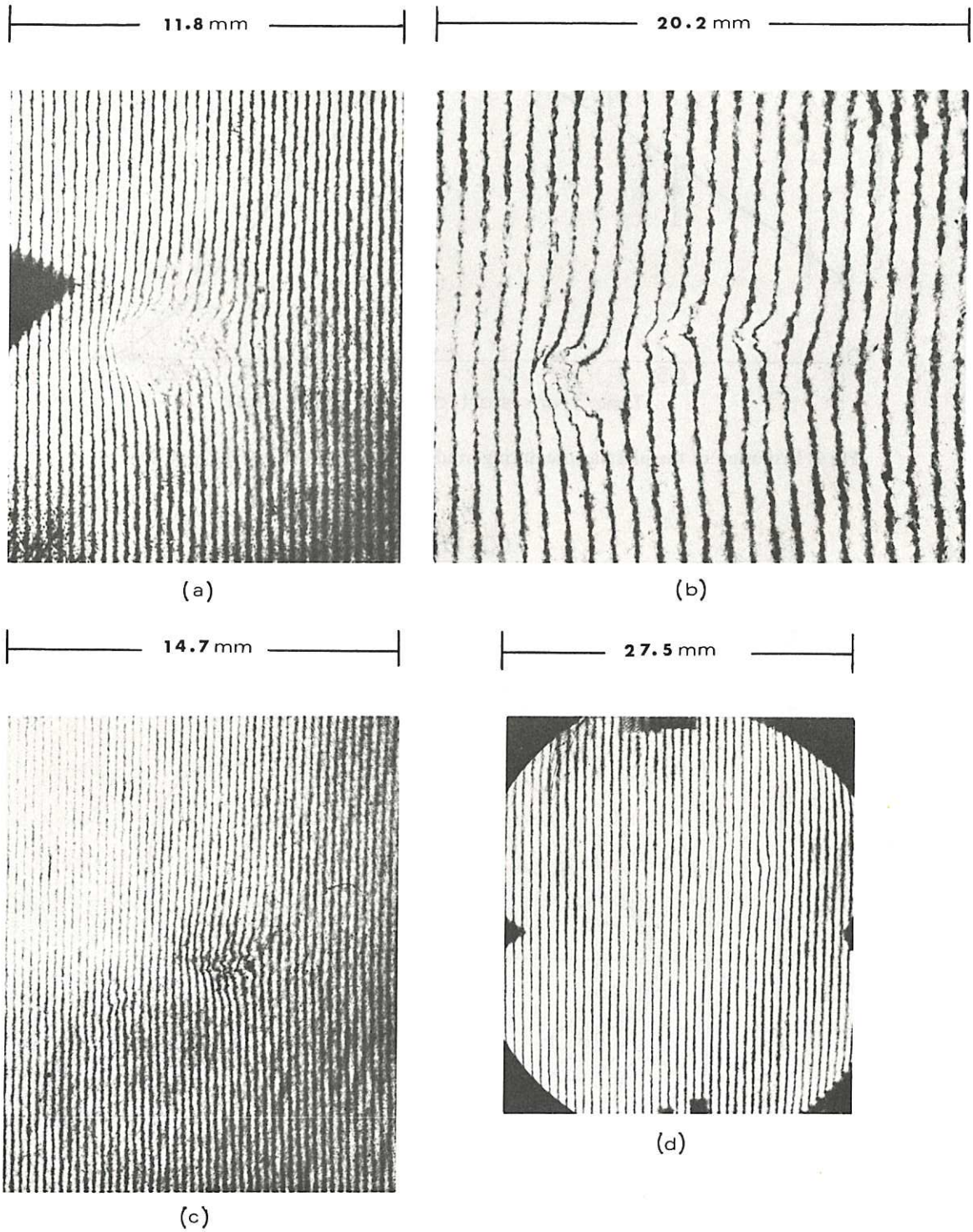

Fig.5 Interferograms of D_2 plasma: (a) 0·7 μs, (b) 1·2 μs, (c) 1·7 μs, (d) 2·8 μs from start of TROJAN pulse (CO_2 laser incident from left).

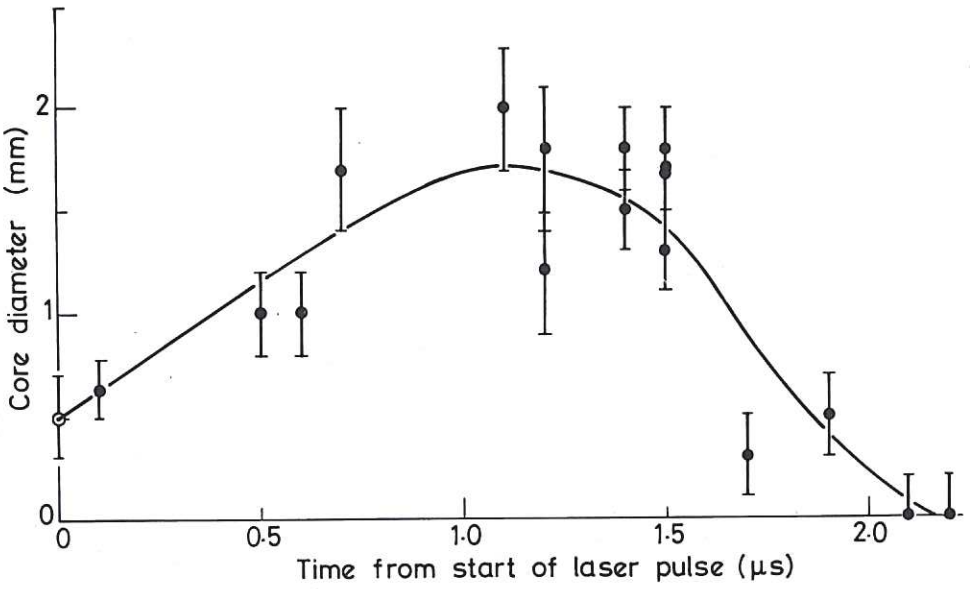

Fig.6 Evolution of the plasma core during irradiation by a 1·3kJ TROJAN pulse.

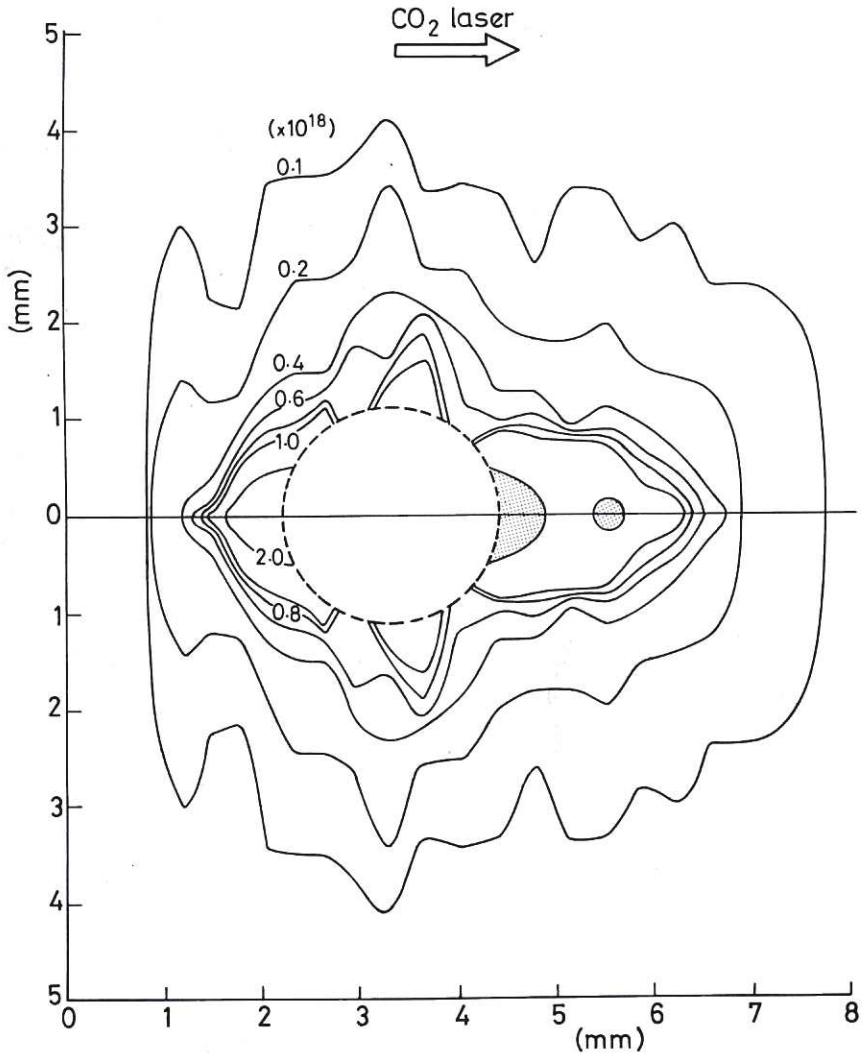

Fig.7 Electron isodensity contour map corresponding to the interferogram given in Fig.5(a). The dotted circle indicates the limit of measureable fringes while the shaded regions are dominated by neutral material.

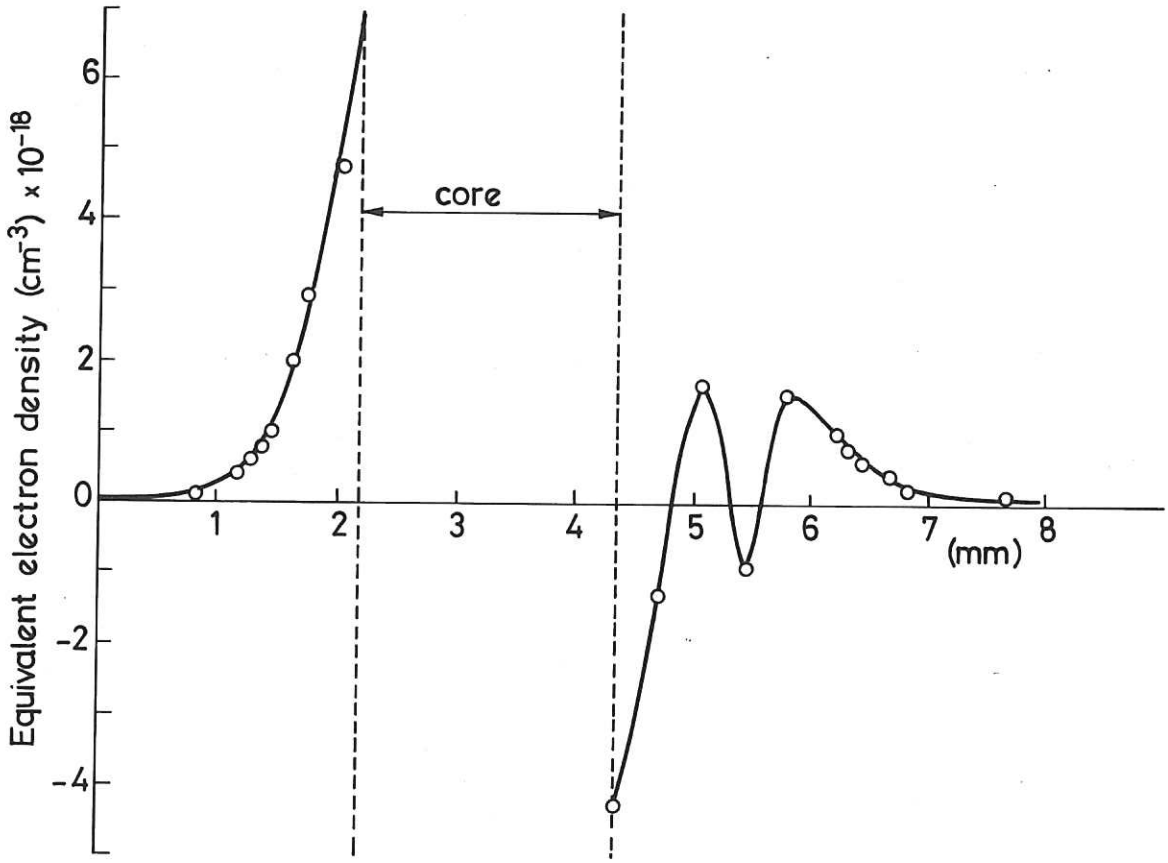

Fig.8 Electron density profile obtained from Fig.7 for a scan along the symmetry axis of the plasma. Negative electron densities indicate regions dominated by neutral material.

HER MAJESTY'S STATIONERY OFFICE

Government Bookshops

49 High Holborn, London WC1V 6HB
13a Castle Street, Edinburgh EH2 3AR
41 The Hayes, Cardiff CF1 1JW
Brazennose Street, Manchester M60 8AS
Wine Street, Bristol BS1 2BQ
258 Broad Street, Birmingham B1 2HE
80 Chichester Street, Belfast BT1 4JY

Government publications are also available through booksellers